

Fabrication and Characterization of Y Doped ZnO Thin Films

Deepak Chaudhary¹, Tarun Kumar² And Dr. Amit Kumar³

Ph.D Scholar, Department of Physics, SRU Alwar(Raj.), India¹

Lecturer, Department of Physics, Government Polytechnic, Sutawali, Amroha(UP), India²

Professor, Department of Physics, IET Alwar, (Raj.), India³

Corresponding Author: Deepak Chaudhary

ABSTRACT: no thin films were deposited on glass substrates at different Zinc concentration and their effects on structural properties were investigated. Zinc acetate dehydrate was used as the solvent. The molar ratio of Monoethanolamine to Zinc acetate was maintained as 1. The crystal structure and orientation of the films were analyzed by XRD. The XRD patterns show that the ZnO films are polycrystalline with wurtzite hexagonal structure. The film with 0.5 m/l concentration has the better crystallinity. The thickness of the films was determined by thickness Profilometer. The surface morphology of the films was observed by Scanning electron microscope. The SEM images show that they are homogeneous, continuous and spindle like shape.

KEYWORDS: ZnO Thin Films, XRD, SEM.

Date of Submission: 12-02-2018

Date of acceptance: 27-02-2018

I. Introduction

Zinc oxide (ZnO) is one of the II-VI oxide semiconductors with hexagonal wurtzite structure. It is an attractive candidate instead of GaN for short wavelength optoelectronic devices because of its wide band gap ($E_g = 3.37$ eV) and high exciton binding energy (60 MeV). In addition, ZnO can be extensively studied in surface acoustic wave devices, non-linear optical devices and photovoltaic equipment[1].

ZnO thin films were fabricated, using the spray pyrolysis method, on glass substrates at different temperatures deposition varying from 350 to 550°C. SEM analysis revealed that the surface morphology of the so-obtained films is uniform and evolves with the substrate temperature during the growth. Mainly, the grain size increases and the surface of the films become rougher with the increase of the substrate temperature to 550 °C. The optical properties were discussed from the effect of substrate temperature[4]. All ZnO films show a high average transmittance above 80% in the visible range of the optical spectrum. The optical band gap value of the films increases when substrate temperature increases, attributed to the decrease of the disorder in the material[8]. For all samples, the photoluminescence emission spectra shows a narrow and sharp peak around 383nm, assigned to the exciton recombination, and a broad band emission in the visible range, attributed to defects forming deep energy levels in the band gap. The intensity of the UV peaks of ZnO thin film increased whereas the visible emission decreased with the increase of the substrate temperature in the growth process. This phenomenon corroborates the highest quality of the ZnO thin film achieve when the film is prepared at an optimized temperature equal to 550 °C .

Crystal structure of Zinc oxide[2] .

Zinc oxide naturally crystallizes in Wurtzite structure which belong to the space group P6₃mc. The Wurtzite structure is a hexagonal lattice in which each Zn²⁺ ion is tetrahedrally bonded to four O²⁻ ions and vice-versa; this is shown in below figure. In this structure the Zn terminated face (0001) and O terminated face (0001) are the polar faces while the non-polar faces are (1120) and (1010) which contain equal number of Zinc and Oxygen atoms. The plane perpendiculars to the c-axis are called basal planes. Thus there is a polar symmetry along the hexagonal axis[11]. This gives rise to piezoelectricity in ZnO and also plays key role in its crystal growth. The tetrahedral coordination of ZnO indicates the presence of sp³ hybridized covalent bonding, but the strong ionic character of the Zn-O bond, makes ZnO behave like both covalent and ionic compound. The lattice parameters of hexagonal unit cell $a = 3.2495 \text{ \AA}$ and $c = 5.2069 \text{ \AA}$ [7].

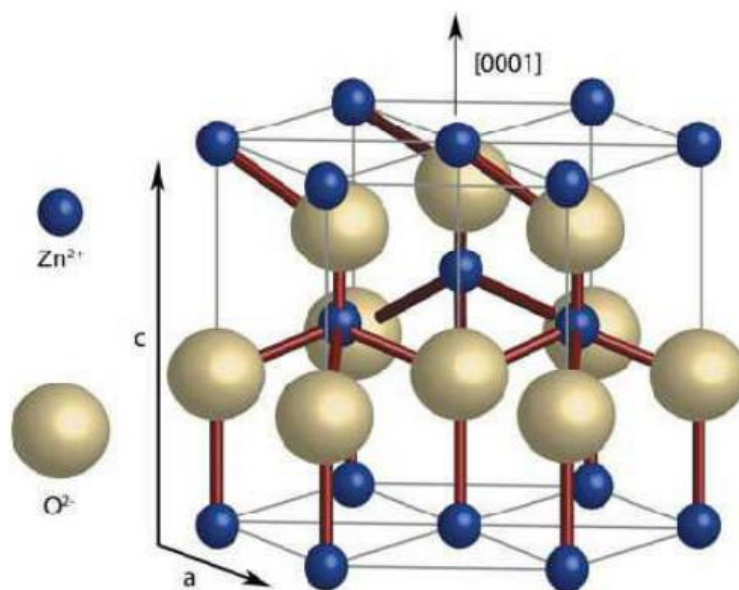


Figure1: Basic structure of ZnO

II. Experimental

Further structural analysis of ZnO films grown on graphene layers was performed using TEM. A cross-sectional TEM image of epitaxial ZnO films grown on graphene layers, which was taken near the 1100 zone axis with $g=11\bar{2}0$. Although this two-beam dark field (DF) image clearly shows edge-type threading dislocations within ZnO films, similar to those of the ZnO layers grown on single crystalline sapphire substrates, [16,17] the ZnO films have no significant microstructural defects, such as voids or cracks. Furthermore, the corresponding selective area electron diffraction (SAED) pattern exhibited a regular spot array, indicating the ZnO films were single crystalline at the measured area of 800 nm in diameter [13].

Because the deep-level emission is usually ascribed to oxygen vacancy defects, a weak deep-level emission signifies the high crystalline quality of the ZnO film. X-ray diffraction (XRD) relies on the dual wave/particle nature of X-rays to obtain information about the structure of crystalline materials. A primary use of the technique is the identification and characterization of compounds based on their diffraction pattern [17].

The dominant effect that occurs when an incident beam of monochromatic X-rays interacts with a target material is scattering of those X-rays from atoms within the target material. In materials with regular structure (i.e. crystalline), the scattered X-rays undergo constructive and destructive interference. This is the process of diffraction. The diffraction of X-rays by crystals is described by Bragg's Law, $n(\lambda) = 2d \sin(\theta)$ [14]. The directions of possible diffractions depend on the size and shape of the unit cell of the material. The intensities of the diffracted waves depend on the kind and arrangement of atoms in the crystal structure. However, most materials are not single crystals, but are composed of many tiny crystallites in all possible orientations called a polycrystalline aggregate or powder. When a powder with randomly oriented crystallites is placed in an X-ray beam, the beam will see all possible interatomic planes. If the experimental angle is systematically changed, all possible diffraction peaks from the powder will be detected [15].

III. Results And Discussion

(i) SEM results of Y doped ZnO thin films

FE-SEM images of the surface and cross-section of yttrium-doped ZnO thin films prepared during the first post-heat treatment with different doping concentrations. It is found that the Y doping concentration has a significant influence on the surface morphology of the ZnO thin films. The pure ZnO thin film (a) is composed of close-packed nanoparticles, arrayed regularly on the substrate with a narrow distribution of grain sizes. For the doped ZnO thin film, some agglomerated grains and a porous structure were observed; moreover, the similar morphology was more obvious with increasing yttrium doping concentration. This may be due to the formation of stresses by the difference in the ionic radii between zinc and yttrium. Columnar ZnO crystals, which grew together between layers and layers and formed a serial whole, and the film's thickness of about 300 nm were observed in the cross-section image of the film (f) shown in Figure 2.

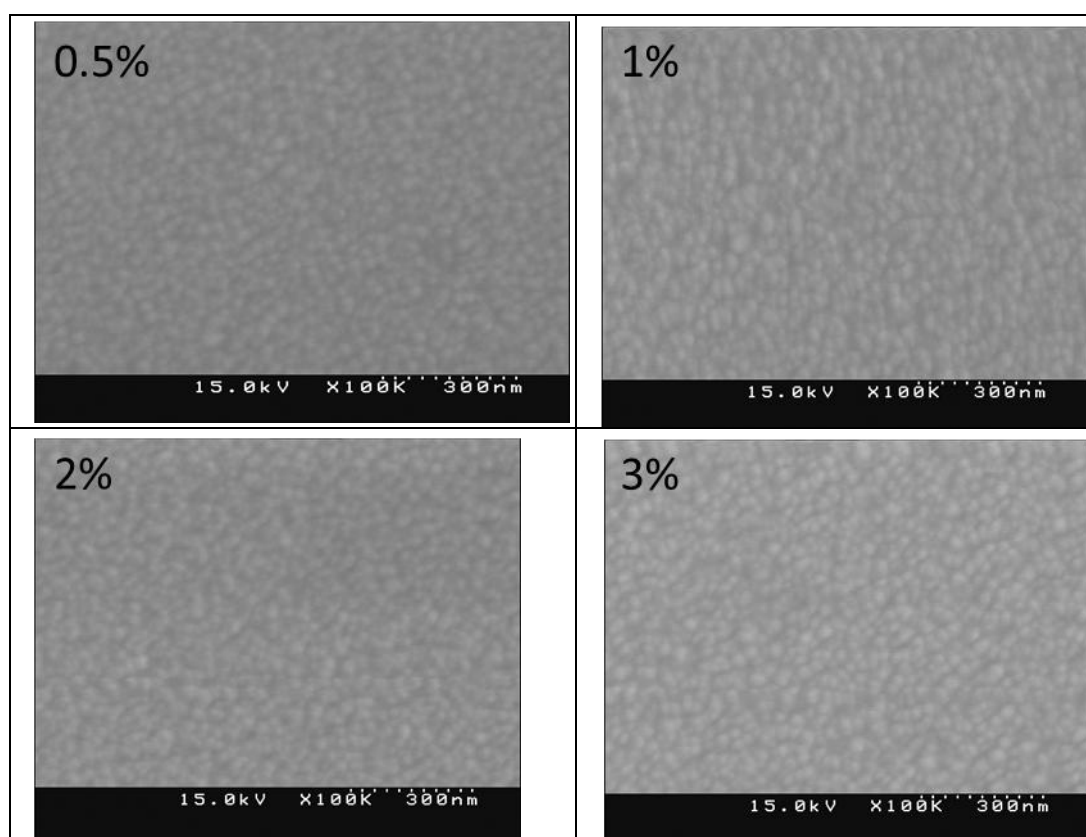


Figure 2: FE-SEM images of the surface and cross-section of yttrium-doped ZnO thin films prepared during the first post-heat treatment with different doping concentrations

(ii) XRD results of Y doped ZnO thin films

XRD patterns of the pure and yttrium-doped ZnO thin films with the first post-heat treatment. The inset shows the values of the lattice constant c of the samples at different doping concentrations. The unit of the lattice constant c is Angstrom. Figure(3) shows XRD patterns of the pure and doped ZnO thin films prepared during the first post-heat treatment with different yttrium concentrations (0.5, 1, 3 and 5 at%) on glass substrates. All the ZnO thin films exhibit the preferred(0 0 2) orientation. This indicates that the c -axis of the grains becomes uniformly perpendicular to the substrate surface, suggesting that the surface energy of the (0 0 2) plane is the lowest in ZnO crystal [16]. No yttrium oxide phases were observed, which means that some Y^{3+} ions would uniformly substitute into the Zn^{2+} sites or interstitial sites in the ZnO lattice. The peak intensities of those films decreased with increasing doping concentrations, which indicates that an increase in doping concentrations deteriorates the crystalline of films. In addition, compared with the pure ZnO thin film, increasing yttrium concentrations caused the position shift of the doped ZnO thin films' (0 0 2) peak to lower diffraction angles. Correspondingly, the c -axis lattice constants of the thin films increased from 5.205 to 5.247 Å with increasing yttrium concentration, as shown in the inset of figure 3. This may be due to the fact that the ionic radius Y^{3+} (0.89 Å) is larger than that of Zn^{2+} (0.74 Å). The variation of the c -axis lattice constant further suggests that Y^{3+} ions replace the Zn^{2+} lattice sites or interstitial sites in the films.

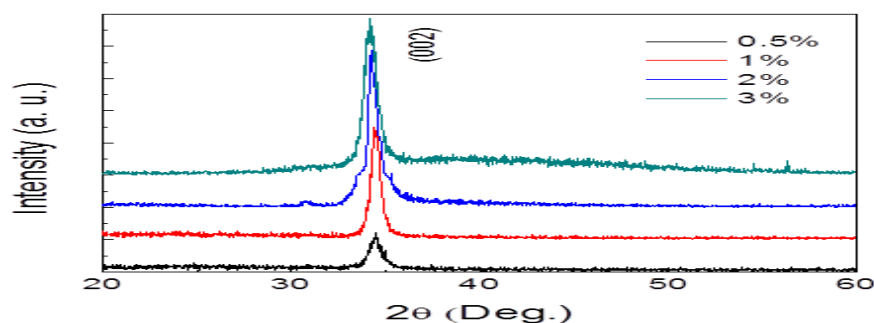


Figure3: XRD results of Y doped ZnO thin films

IV. Conclusion

ZnO thin films were prepared with different Zinc concentration and their effects on structural, morphology and optical properties were studied. The XRD results show that the films are polycrystalline wurtzite hexagonal structure and have no preferred orientation. The film with 0.5 m/l concentration has minimum value of strain and has larger particle size compared to other concentrations. Zinc oxide is one of the most important n-type semi-conductor intensively utilized in solar cells, transparent conducting electrodes and opto-electronic devices.

References

- [1]. [1] Y.J. Lee, D.S. Ruby, D.W. Peters, B.B. McKenzie, J.W.P. Hsu ZnO nanostructures as efficient antireflection layers in solar cells Nano. Lett., 8 (2008), pp. 1501-1505
- [2]. [2] I. Gonzalez-Valls, M. Lira-Cantu Vertically-aligned nanostructures of ZnO for excitonic solar cells: a review Energy Environ. Sci., 2 (2009), pp. 19-34
- [3]. [3] Y.J. Lee, D.S. Ruby, D.W. Peters, B.B. McKenzie, J.W.P. Hsu ZnO Nanostructures as Efficient Antireflection Layers for Solar Cells Nano Lett., 8 (2008), pp. 1501-1505
- [4]. [4] J.Y. Chen, K.W. Sun Growth of vertically aligned ZnO nanorod arrays as antireflection layer on silicon solar cells. Sol Energy Mater. Sol. Cells., 94 (2010), pp. 930-934
- [5]. [5] F.C. Krebs, S.A. Gevorgyan, J.A. Alstrup roll-to-roll process to flexible polymer solar cells: model studies, manufacture and operational stability studies J. Mater. Chem., 19 (2009), pp. 5442-5451
- [6]. [6] F.C. Krebs Air stable polymer photovoltaics based on a process free from vacuum steps and fullerenes Sol. Energy Mater. Sol. Cells., 92 (2008), pp. 715-726
- [7]. [7] T. Shirakawa, T. Umeda, Y. Hashimoto, A. Fujii, K. Yoshino Effect of ZnO layer on characteristics of conducting polymer/C60 photovoltaic cell J. Phys. D: Appl. Phys., 37 (2004), pp. 847-850
- [8]. [8] C.H. Hsieh, Y.J. Cheng, P.J. Li, C.H. Chen, M. Dubosc, R.M. Liang, C.S. Hsu Highly efficient and stable inverted polymer solar cells integrated with a cross-linked fullerene material as an interlayer J. Am. Chem. Soc., 132 (2010), pp. 4887-4893
- [9]. [9] B.L. Zhu, X.H. Sun, X.Z. Zhao, F.H. Su, G.H. Li, X.G. Wu, J. Wu, R. Wu, J. Liu The effects of substrate temperature on the structure and properties of ZnO films prepared by pulsed laser deposition Vacuum, 82 (2008), pp. 495-500
- [10]. [10] M. Bouderbala, S. Hamzaoui, B. Amrani, A.H. Reshak, M. Adnane, T. Sahraoui, M. Zerdali Thickness dependence of structural, electrical and optical behaviour of undoped ZnO thin films. Physica B, 403 (2008), pp. 3326-3330
- [11]. [11] A. Bedia, F.Z. Bedia, M. Aillerie, N. Maloufi, S. OuldSaadHamady, O. Perroud, B. Benyoucef Optical, electrical and structural properties of nano-pyramidal ZnO films grown on glass substrate by spray pyrolysis technique Opt. Mater., 36 (2014), pp. 1123-1130
- [12]. [12] S. Ilican, M. Caglar, Y. Caglar Sn doping effects on the electro-optical properties of sol gel derived transparent ZnO films Appl. Surf. Sci., 256 (2010), pp. 7204-7210
- [13]. [13] R. Swanepoel Determination of the thickness and optical constants of amorphous silicon J. Phys. E: Sci. Instrum., 16 (1983), pp. 1214-1222
- [14]. [14] F.Z. Bedia, A. Bedia, N. Maloufi, M. Aillerie, F. Genty, B. Benyoucef Effect of tin doping on optical properties of nanostructured ZnO thin films grown by spray pyrolysis technique J. Alloys Compd., 616 (2014), pp. 312-318
- [15]. [15] F. Zahedi, R.S. Dariani, S.M. Rozati Effect of substrate temperature on the properties of ZnO thin films prepared by spray pyrolysis Mater. Sci. Semicond. Proc., 16 (2013), pp. 245-249
- [16]. [16] I. Soumahoro, G. Schmerber, A. Douayar, S. Colis, M. Abd-Lefdil, N. Hassanain, A. Berrada, D. Muller, A. Slaoui, H. Rinnert, A. Dinia Structural, optical, and electrical properties of Yb-doped ZnO thin films prepared by spray pyrolysis method J. Appl. Phys., 109 (2011), p. 033708
- [17]. [17] Amit Kumar, Manoj Kumar, Beer Pal Singh "Fabrication and characterization of magnetron sputtered arsenic doped p-type ZnO epitaxial thin films" in International Journal Applied Surface Science vol-256 7200-7203, APSUSC202181-4, Elsevier, 2010

International Journal of Engineering Science Invention (IJESI) is UGC approved Journal with Sl. No. 3822, Journal no. 43302.

Deepak Chaudhary. "Fabrication and Characterization of Y Doped ZnO Thin Films" International Journal of Engineering Science Invention (IJESI), vol. 07, no. 02, 2018, pp. 26-29.